Supplementary Information for

Harvesting forage fish can prevent fishing-induced population collapses of large piscivorous fish

Floor H. Soudijn, P. Daniël van Denderen, Mikko Heino, Ulf Dieckmann, André M. de Roos

Floor H. Soudijn.
E-mail: floor.soudijn@wur.nl

This PDF file includes:

Appendix A. Community-dynamics model

Model description. The community-dynamics model follows the bioenergetics approach introduced by Yodzis & Innes (1), which was extended to a stage-structured version by de Roos et al. (2). The full system of equations can be found at the end of this section, Eq. (6-31). We describe all modeled processes in detail, in terms of mass-specific process rates.

Food ingestion takes place following a Holling Type II functional response as a function of the encountered food density E, and the net-biomass production per unit body mass is

$$\nu(E) = \sigma \frac{I\,E}{H+E} - T. \quad [1]$$

The food ingestion depends on the maximum ingestion rate I and the half-saturation density H. Ingested food is assimilated with conversion efficiency σ. Subsequently, the energy is used to cover the mass-specific somatic maintenance costs T. The food-encounter rate E is different for all stages of clupeids and cod, as it depends on their feeding preferences for different resources and the resource densities (see below). When the assimilated energy exceeds the somatic maintenance costs, the net-biomass production is invested in somatic growth by juveniles, split between somatic growth and reproduction by small adults, and invested in reproduction by large adults. Under starvation conditions, the net-biomass production rate becomes negative, somatic growth and maturation stops, and no energy is invested in reproduction. The net-biomass production rate restricted to positive values is denoted by

$$\nu^{+}(E) = \begin{cases} \nu(E), & \text{if} \quad \nu(E) > 0, \\ 0, & \text{otherwise.} \end{cases} \quad [2]$$

The transition rate between stages is based on the derivation decribed by Soudijn & de Roos (3). It translates individual-level assumptions about energy expenditure into a population-level transition rate per unit biomass,

$$\gamma(\nu, d) = \begin{cases} \dfrac{\kappa\,\nu - d}{1 - z^{1-\frac{d}{\kappa\,\nu}}}, & \text{if} \quad \nu > 0, \\ 0, & \text{otherwise.} \end{cases} \quad [3]$$

The transition rate from one stage to the next is restricted to positive values of the net-biomass production rate ν and depends on the mortality rate d and the ratio z between the body sizes at the beginning and end of a stage. The transition rate further depends on the fraction κ of energy invested in somatic growth. The energy that is not invested in somatic growth (i.e., the fraction $1-\kappa$) is allocated to reproduction. Reproductive energy is stored throughout the growing season. For the small-adult stage, the transition rate above also describes the transfer rate of the reproductive storage to the large-adult stage.

Mortality d is comprised of background mortality μ, starvation mortality, fishing mortality F and predation mortality P. Background mortality is size-independent, affecting all individuals equally. Starvation mortality occurs when the food intake is not sufficient to cover the somatic maintenance costs. Fishing mortality and predation mortality are stage- and species-specific. This results in the following general expressions for the mortality rates of cod and clupeids, respectively, d_{C} and d_{S}:

$$d_{\mathrm{C}}(E) = \begin{cases} \mu + F - \nu(E), & \text{if} \quad \nu(E) < 0, \\ \mu + F, & \text{otherwise,} \end{cases} \quad [4]$$

$$d_{\mathrm{S}}(E) = \begin{cases} \mu + F + P - \nu(E), & \text{if} \quad \nu(E) < 0, \\ \mu + F + P, & \text{otherwise.} \end{cases} \quad [5]$$

Note that the actual expressions are stage-specific as they depend on stage-specific values of F, P and $\nu(E)$. The adult mortality rate also governs losses of the reproductive-energy storages: when adult individuals die, the energy they have stored for reproduction dies with them.

The model is defined in terms of biomasses per volume and consists of a resource for clupeids (R_{S}), a resource for cod juveniles (R_{J}), and a resource for cod adults (R_{A}), together with size-structured clupeid and cod populations. The clupeid population is divided in one juvenile stage (S_{J}), two adult stages (S_{A} and S_{B}), and their reproductive storages (Sg_{A} and Sg_{B}). The cod population is divided in one juvenile stage (C_{J}), two adult stages (C_{A} and C_{B}), and their reproductive storages (Cg_{A} and Cg_{B}). Clupeids forage on the clupeid resource throughout their life, and the food-encounter rate is thus equal for all clupeid stages (Table S1). Cod switches diet, and the food-encounter rate in each cod stage depends on the biomass density and stage-specific foraging preference β for the corresponding food source. Predation of clupeids by cod reduces clupeid somatic biomass and the reproductive-energy storages of adult clupeid stages simultaneously. The resource grazing rates G and stage-specific functions for food-encounter rates E and predation rates P are listed in Table S1. Foraging preferences of the cod stages for the different food sources are listed in Table S4.

The continuous-time dynamics over time t during the growing season ($0 \leq t < Y$, where Y denotes the growing season's duration) are described by the following set of ordinary differential equations:

$$\frac{dR_{\mathrm{S}}}{dt} = \delta(R_{\mathrm{S}_{\max}} - R_{\mathrm{S}}) - G_{\mathrm{S}}\, R_{\mathrm{S}}, \quad [6]$$

$$\frac{dR_{\mathrm{J}}}{dt} = \delta(R_{\mathrm{J}_{\max}} - R_{\mathrm{J}}) - G_{\mathrm{J}}\, R_{\mathrm{J}}, \quad [7]$$

$$\frac{dR_{\mathrm{A}}}{dt} = \delta(R_{\mathrm{A}_{\max}} - R_{\mathrm{A}}) - G_{\mathrm{A}}\, R_{\mathrm{A}}, \quad [8]$$

$$\frac{dS_{\mathrm{J}}}{dt} = \nu^{+}_{\mathrm{S_J}}(E_{\mathrm{S}})\, S_{\mathrm{J}} - \gamma_{\mathrm{S_J}}(\nu_{\mathrm{S_J}}(E_{\mathrm{S}}), d_{\mathrm{S_J}}(E_{\mathrm{S}}))\, S_{\mathrm{J}} - d_{\mathrm{S_J}}(E_{\mathrm{S}})\, S_{\mathrm{J}}, \quad [9]$$

$$\frac{dS_{\mathrm{A}}}{dt} = \gamma_{\mathrm{S_J}}(\nu_{\mathrm{S_J}}(E_{\mathrm{S}}), d_{\mathrm{S_J}}(E_{\mathrm{S}}))\, S_{\mathrm{J}} + \kappa\, \nu^{+}_{\mathrm{S_A}}(E_{\mathrm{S}})\, S_{\mathrm{A}} - \gamma_{\mathrm{S_A}}(\nu_{\mathrm{S_A}}(E_{\mathrm{S}}), d_{\mathrm{S_A}}(E_{\mathrm{S}}))\, S_{\mathrm{A}} - d_{\mathrm{S_A}}(E_{\mathrm{S}})\, S_{\mathrm{A}}, \quad [10]$$

$$\frac{dS_{\mathrm{B}}}{dt} = \gamma_{\mathrm{S_A}}(\nu_{\mathrm{S_A}}(E_{\mathrm{S}}), d_{\mathrm{S_A}}(E_{\mathrm{S}}))\, S_{\mathrm{A}} - d_{\mathrm{S_B}}(E_{\mathrm{S}})\, S_{\mathrm{B}}, \quad [11]$$

$$\frac{dSg_{\mathrm{A}}}{dt} = (1-\kappa)\, \nu^{+}_{\mathrm{S_A}}(E_{\mathrm{S}})\, S_{\mathrm{A}} - \gamma_{\mathrm{S_A}}(\nu_{\mathrm{S_A}}(E_{\mathrm{S}}), d_{\mathrm{S_A}}(E_{\mathrm{S}}))\, Sg_{\mathrm{A}} - d_{\mathrm{S_A}}(E_{\mathrm{S}})\, Sg_{\mathrm{A}}, \quad [12]$$

$$\frac{dSg_{\mathrm{B}}}{dt} = \gamma_{\mathrm{S_A}}(\nu_{\mathrm{S_A}}(E_{\mathrm{S}}), d_{\mathrm{S_A}}(E_{\mathrm{S}}))\, Sg_{\mathrm{A}} + \nu^{+}_{\mathrm{S_B}}(E_{\mathrm{S}})\, S_{\mathrm{B}} - d_{\mathrm{S_B}}(E_{\mathrm{S}})\, Sg_{\mathrm{B}}, \quad [13]$$

$$\frac{dC_{\mathrm{J}}}{dt} = \nu^{+}_{C_{\mathrm{J}}}(E_{\mathrm{C_J}})\, C_{\mathrm{J}} - \gamma_{\mathrm{C_J}}(\nu_{\mathrm{C_J}}(E_{\mathrm{C_J}}), d_{\mathrm{C_J}}(E_{\mathrm{C_J}}))\, C_{\mathrm{J}} - d_{\mathrm{C_J}}(E_{\mathrm{C_J}})\, C_{\mathrm{J}}, \quad [14]$$

$$\frac{dC_{\mathrm{A}}}{dt} = \gamma_{\mathrm{C_J}}(\nu_{\mathrm{C_J}}(E_{\mathrm{C_J}}), d_{\mathrm{C_J}}(E_{\mathrm{C_J}}))\, C_{\mathrm{J}} + \kappa\, \nu^{+}_{\mathrm{C_A}}(E_{\mathrm{C_A}})\, C_{\mathrm{A}} - \gamma_{\mathrm{C_A}}(\nu_{\mathrm{C_A}}(E_{\mathrm{C_A}}), d_{\mathrm{C_A}}(E_{\mathrm{C_A}}))\, C_{\mathrm{A}} - d_{\mathrm{C_A}}(E_{\mathrm{C_A}})\, C_{\mathrm{A}}, \quad [15]$$

$$\frac{dC_{\mathrm{B}}}{dt} = \gamma_{\mathrm{C_A}}(\nu_{\mathrm{C_A}}(E_{\mathrm{C_A}}), d_{\mathrm{C_A}}(E_{\mathrm{C_A}}))\, C_{\mathrm{A}} - d_{\mathrm{C_B}}(E_{\mathrm{C_B}})\, C_{\mathrm{B}}, \quad [16]$$

$$\frac{dCg_{\mathrm{A}}}{dt} = (1-\kappa)\, \nu^{+}_{\mathrm{C_A}}(E_{\mathrm{C_A}})\, C_{\mathrm{A}} - \gamma_{\mathrm{C_A}}(\nu_{\mathrm{C_A}}(E_{\mathrm{C_A}}), d_{\mathrm{C_A}}(E_{\mathrm{C_A}}))\, Cg_{\mathrm{A}} - d_{\mathrm{C_A}}(E_{\mathrm{C_A}})\, Sg_{\mathrm{A}}, \quad [17]$$

$$\frac{dCg_{\mathrm{B}}}{dt} = \gamma_{\mathrm{C_A}}(\nu_{\mathrm{C_A}}(E_{\mathrm{C_A}}), d_{\mathrm{C_A}}(E_{\mathrm{C_A}}))\, Cg_{\mathrm{A}} + \nu^{+}_{\mathrm{C_B}}(E_{\mathrm{C_B}})\, C_{\mathrm{B}} - d_{\mathrm{C_B}}(E_{\mathrm{C_B}})\, Sg_{\mathrm{B}}. \quad [18]$$

When the growing season ends, reproduction takes place instantaneously at times $t_n = nY$ with $n = 1, 2, \ldots$. Below, we denote the times just before and just after t_n by, respectively, t_n^- and t_n^+:

$$R_{\mathrm{S}}(t_n^+) = R_{\mathrm{S}}(t_n^-), \quad [19]$$
$$R_{\mathrm{J}}(t_n^+) = R_{\mathrm{J}}(t_n^-), \quad [20]$$
$$R_{\mathrm{A}}(t_n^+) = R_{\mathrm{A}}(t_n^-), \quad [21]$$

$$S_{\mathrm{J}}(t_n^+) = S_{\mathrm{J}}(t_n^-) + Sg_{\mathrm{A}}(t_n^-) + Sg_{\mathrm{B}}(t_n^-), \quad [22]$$
$$S_{\mathrm{A}}(t_n^+) = S_{\mathrm{A}}(t_n^-), \quad [23]$$
$$S_{\mathrm{B}}(t_n^+) = S_{\mathrm{B}}(t_n^-), \quad [24]$$
$$Sg_{\mathrm{A}}(t_n^+) = 0, \quad [25]$$
$$Sg_{\mathrm{B}}(t_n^+) = 0, \quad [26]$$

$$C_{\mathrm{J}}(t_n^+) = C_{\mathrm{J}}(t_n^-) + Cg_{\mathrm{A}}(t_n^-) + Cg_{\mathrm{B}}(t_n^-), \quad [27]$$
$$C_{\mathrm{A}}(t_n^+) = C_{\mathrm{A}}(t_n^-), \quad [28]$$
$$C_{\mathrm{B}}(t_n^+) = C_{\mathrm{B}}(t_n^-), \quad [29]$$
$$Cg_{\mathrm{A}}(t_n^+) = 0, \quad [30]$$
$$Cg_{\mathrm{B}}(t_n^+) = 0. \quad [31]$$

During a reproductive event, biomass in the reproductive-energy storages is transformed into juveniles, for both clupeids (22) and cod (27). At the same moment, the reproductive-energy storages are thus set to zero (25, 26, 30, 31), while the resource biomasses (19 - 21) and the adult somatic biomasses (23, 24, 28, 29) do not change.

Model parameterization. All parameter values are derived from individual-level data; no population-level data are used for parameterization. Specific parameter values are determined for each fish stage, based on the average body mass in the stage. We test the effects of a range of values for cod and clupeid fishing mortalities on the model dynamics. The model parameterization is based on the study by van Leeuwen et al. (4), except for the parameter values describing seasonal reproduction and fishing of the clupeids. Body sizes, energetic parameters, and mortality parameters for each fish stage can be found in Table S2. Foraging preferences of the cod stages for the different fish and non-fish resources are listed in Table S4. Species-specific and system parameters can be found in Table S3.

Fishing is implemented as a size-dependent process: it affects small individuals less than large individuals. For trawl and gill-net fishing, juvenile-cod fisheries retention (at age 1 year) is estimated to be 2% of adult-cod fisheries retention (at ages 3-7 years) (5). Based on the retention of herring individuals of 3.4 g or about 8 cm (6) in trawling nets with a small mesh size, juvenile-clupeid fisheries retention is estimated at 26.4% (7) of adult-clupeid fisheries retention. Yet, since this estimate increases to 50% for herring individuals that are only 1 cm larger, we use a conservative value of 50%. The fisheries yield for cod is calculated based on the catch of only adult individuals because there is a minimum allowable landing size of 38 cm for cod (8). In contrast, the fisheries yield for clupeids is calculated based on the catch of both juveniles and adults as there are no regulations stipulating a minimum allowable landing size of Baltic sprat and herring.

The length of the growing season is set to $Y = 250$ days. It is assumed that all considered processes (somatic maintenance, food intake, and mortality) decrease to negligible levels during winter. The dynamics are thereby effectively compressed from 365 to 250 days. For the sake of simplicity, the spawning of cod and clupeids are modeled to occur instantaneously and simultaneously at the end of the growing season. The peak-spawning time of clupeids has been relatively constant over the years, ocurring at the end of May or the beginning of June (9, 10). The peak-spawning time of cod has been more variable, generally ocurring between mid-May and the beginning of July. Both species spawn over a period of about 90 days (9, 10).

The use of a dimensionless constant for the half-saturation density H stems from the argument that both the maximum ingestion rate and the attack rate scale with body size with the same factor (4). Rescaling of the value of H to 1 g/Vol affects the reference volume of all the calculations in the model. Recent studies show that a general value of 3 mg/L can be assumed for H (11). This value of H corresponds to a reference volume of Vol = 333 L for our calculations. We thus transform the values of biomasses per volume predicted by our model in the unit g/Vol to the unit g/L by multiplying them with 0.003 Vol/L.

Model analysis. Model analysis is based on numerical simulations using publicly available C-based simulation programs (model code is publicly accessible at 10.5281/zenodo.3779839). Parameter dependencies are studied by the integrating model dynamics over long time periods of 50,000 days while varying the considered parameter value in small steps (see box 3.5 in 11 for an explanation of this procedure to study parameter dependencies). Time averages of the model variables are calculated over the last 60% of the 50,000 day time periods.

Table S1. Functions describing the encounter rates, predation rates, and grazing rates.

Description	Function
Cod population	
Juvenile food-encounter rate	$E_{\mathrm{C_J}} = \beta_{\mathrm{C_J R_J}} R_{\mathrm{J}} + \beta_{\mathrm{C_J S_J}} S_{\mathrm{J}}$
Small-adult food-encounter rate	$E_{\mathrm{C_A}} = \beta_{\mathrm{C_A R_A}} R_{\mathrm{A}} + \beta_{\mathrm{C_A S_A}} (S_{\mathrm{A}} + Sg_{\mathrm{A}}) + \beta_{\mathrm{C_A S_B}} (S_{\mathrm{B}} + Sg_{\mathrm{B}})$
Large-adult food-encounter rate	$E_{\mathrm{C_B}} = \beta_{\mathrm{C_B R_A}} R_{\mathrm{A}} + \beta_{\mathrm{C_B S_A}} (S_{\mathrm{A}} + Sg_{\mathrm{A}}) + \beta_{\mathrm{C_B S_B}} (S_{\mathrm{B}} + Sg_{\mathrm{B}})$
Clupeid population	
Food-encounter-rate	$E_{\mathrm{S}} = R_{\mathrm{S}}$
Predation rate on juveniles	$P_{\mathrm{S_J}} = I_{\mathrm{C_J}} \frac{\beta_{\mathrm{C_J S_J}}}{H + E_{\mathrm{C_J}}} C_{\mathrm{J}} + I_{\mathrm{C_A}} \frac{\beta_{\mathrm{C_A S_J}}}{H + E_{\mathrm{C_A}}} C_{\mathrm{A}} + I_{\mathrm{C_B}} \frac{\beta_{\mathrm{C_B S_J}}}{H + E_{\mathrm{C_B}}} C_{\mathrm{B}}$
Predation rate on small adults	$P_{\mathrm{S_A}} = I_{\mathrm{C_A}} \frac{\beta_{\mathrm{C_A S_A}}}{H + E_{\mathrm{C_A}}} C_{\mathrm{A}} + I_{\mathrm{C_B}} \frac{\beta_{\mathrm{C_B S_A}}}{H + E_{\mathrm{C_B}}} C_{\mathrm{B}}$
Predation rate on large adults	$P_{\mathrm{S_B}} = I_{\mathrm{C_A}} \frac{\beta_{\mathrm{C_A S_B}}}{H + E_{\mathrm{C_A}}} C_{\mathrm{A}} + I_{\mathrm{C_B}} \frac{\beta_{\mathrm{C_B S_B}}}{H + E_{\mathrm{C_B}}} C_{\mathrm{B}}$
Resources	
Grazing rate of clupeid resource	$G_{\mathrm{R_S}} = I_{\mathrm{S_J}} \frac{1}{H + E_{\mathrm{S}}} S_{\mathrm{J}} + I_{\mathrm{S_A}} \frac{1}{H + E_{\mathrm{S}}} S_{\mathrm{A}} + I_{\mathrm{S_B}} \frac{1}{H + E_{\mathrm{S}}} S_{\mathrm{B}}$
Grazing rate of juvenile-cod resource	$G_{\mathrm{R_J}} = I_{\mathrm{C_J}} \frac{\beta_{\mathrm{C_J R_J}}}{H + E_{\mathrm{C_J}}} C_{\mathrm{J}}$
Grazing rate of adult-cod resource	$G_{\mathrm{R_A}} = I_{\mathrm{C_A}} \frac{\beta_{\mathrm{C_A R_J}}}{H + E_{\mathrm{C_A}}} C_{\mathrm{A}} + I_{\mathrm{C_B}} \frac{\beta_{\mathrm{C_B R_J}}}{H + E_{\mathrm{C_B}}} C_{\mathrm{B}}$

Table S2. Default parameter values for all fish stages (from 4). Note that the values for the maximum ingestion rate I and the somatic maintenance costs T are mass-specific. 'Vol' indicates that the maximum resource densities are defined per unit of reference volume. Since we have rescaled the model parameters by setting the half-saturation density H to 1 g/Vol, the size of this reference volume is undefined (see SI section 'Model parameterization'). Values for the fishing mortalities F_{C}, F_{S} and the fisheries retentions ρ_{C}, ρ_{S} of, respectively, cod and clupeids are shown in table S3.

Description		S_{J}	S_{A}	S_{B}	C_{J}	C_{A}	C_{B}
Initial size (g)	W_{b}	0.55	10.7	15.0	0.35	104	832
Average size (g)	$\bar{W}$	3.4	12.7	15.0	18.2	350	832
Maximum ingestion rate (d^{-1})	I	0.23	0.078	0.078	0.08	0.022	0.022
Half-saturation density (g Vol^{-1})	H	1	1	1	1	1	1
Assimilation efficiency	σ	0.3	0.3	0.3	0.3	0.4	0.4
Somatic maintenance costs (d^{-1})	T	0.032	0.02	0.02	0.015	0.006	0.006
Fraction of energy invested in somatic growth	κ	1	0.8	0.0	1	0.8	0.0
Ratio of initial to final body size	z	0.05	0.7	-	0.003	0.125	-
Background mortality rate (d^{-1})	μ	0.001	0.001	0.001	0.001	0.001	0.001
Fishing mortality rate (d^{-1})	F	$\rho_{\mathrm{S}}\, F_{\mathrm{S}}$	F_{S}	F_{S}	$\rho_{\mathrm{C}}\, F_{\mathrm{C}}$	F_{C}	F_{C}

Table S3. Default values of fisheries parameters and system parameters (from 4, unless indicated otherwise). 'Vol' indicates that the maximum resource densities are defined per unit of reference volume. Since we have rescaled the model parameters by setting the half-saturation density H to 1 g/Vol, the size of this reference volume is undefined (see SI section 'Model parameterization').

Symbol	**Value**	**Unit**	**Description**	**Source**
F_{S}	Varied	d^{-1}	Fishing mortality rate of clupeids	
F_{C}	Varied	d^{-1}	Fishing mortality rate of cod	
ρ_{S}	0.5	-	Fisheries retention of clupeid juveniles	(6), (7)
ρ_{C}	0.02	-	Fisheries retention of cod juveniles	(5)
δ	0.1	d^{-1}	Turnover rate of resources	
$R_{\mathrm{S_{max}}}$	98	g Vol^{-1}	Maximum density of clupeid resource	
$R_{\mathrm{J_{max}}}$	1	g Vol^{-1}	Maximum density of juvenile-cod resource	
$R_{\mathrm{A_{max}}}$	0.75	g Vol^{-1}	Maximum density of adult-cod resource	
Y	250	d	Length of growing season	

Table S4. Foraging preferences of cod stages (from 4).

	β_{C_J}	β_{C_A}	β_{C_B}
R_S	0.0	0.0	0.0
R_J	0.8	0.0	0.0
R_A	0.0	0.5	0.2
S_J	0.2	0.3	0.25
S_A	0.0	0.1	0.3
S_B	0.0	0.1	0.25

Appendix B. Statistical model

Choice of data source. The stock assessments in the RAM Legacy Stock Assessment Database currently represent the best available syntheses of catch data and trawl-survey data that exist to derive estimates of biomasses and fishing mortalities. Commercial catch data tend to go back furthest in time, but typically suffer from sampling bias (as fishermen do not 'sample' in a scientific manner). Scientific trawl-survey data, on the other hand, ideally are less biased, but tend to be noisy and have shorter time horizons. Stock assessments have two advantages: they are normally conducted by local experts, who are best positioned to select and process the available data, and they combine both data sources in a way that takes best advantage of the differential strengths of each data source. We acknowledge that stock assessments are not perfect, but using raw data in the form of commercial catches and/or trawl-survey data is unlikely to mitigate the underlying uncertainties and would likely compound other problems. Below we describe in more detail the (limited) possibilities for deducing biomass estimates from trawl-survey data in more detail ('Alternative data sources' section, Figs. S5 and S6).

Statistical analysis. We examined whether there is a statistical interaction between the effects of forage-fish fishing mortality and piscivore fishing mortality on the decline of piscivore stock biomass through time. We defined fish stocks in the RAM Legacy Stock Assessment Database (12, version 3.0, publicly accessible at www.ramlegacy.org/database) as forage-fish stocks based on the list provided by Essington et al. (13). We extracted information on the trophic level of all fish stocks from FishBase using rfishbase (14). We defined fish stocks as piscivorous when their trophic level exceeds 4.0. All piscivores that are classified as highly migratory species by the United Nations (15) were excluded from the analysis. Highly migratory species are expected to depend on several forage-fish stocks along their migration route, and may be fished at different locations along their migration route. From the remaining piscivores, we selected the fish stocks for which the data spans at least 20 years.

For each piscivore, we selected the period, between 5 and 15 years long, of largest decline in piscivore biomass in the time series (Fig. S1). For each selected period, we calculated the average fishing exploitation rates of the piscivore and the forage fish. For both forage fish and piscivores, we used only fish stocks with data on the fishing exploitation rate (annual catch/biomass) since this information was available for most of the stock pairs and we did not want to mix different measures of fishing mortality. When multiple forage-fish stocks overlap with a single piscivore, aggregate forage-fish fishing exploitation rates were calculated as biomass-weighted averages in each year of the decline period (when the total stock biomasses of the forage fish were not available, their spawning stock biomasses were used instead).

We performed ordinary least-squares multiple regression analyses to evaluate how the piscivore-biomass declines depend on the exploitation rates of piscivores and forage fish. Based on the inspection of model fits, we used the natural logarithm of the biomass ratios. We compared models with and without an interaction term between piscivore and forage-fish fishing mortalities and with only piscivore fishing mortality. We determined the explanatory power of the models based on AIC (Akaike information criterion) scores for model fit. When the AIC scores of models differed by less than 2 AIC units, we selected the model with the fewest parameters as the 'best' model.

Excluded data and robustness tests. We excluded the stocks of North East Atlantic Blue whiting and South Africa kingklip as their biomasses predominantly increased over the time series (Fig. S1, Table S5). One forage fish, Iceland capelin, has extremely high exploitation rates (in some years exceeding 3) that are considered unrealistic; this stock was thus removed from the analysis. The combinations of piscivore stocks and forage-fish stocks used for the analysis are listed in Table S5.

We analyzed all data without the combination of the Southern Blue whiting piscivore stock and the Chilean jack mackerel forage-fish stock. This combination has the highest average fishing exploitation rates for the forage fish and the lowest for the piscivore stock in the dataset. Since it has a particularly strong influence on the interaction model (according to its Cook's distance, Fig. S3), we decided to exclude it from our analysis. The inclusion of this stock combination considerably reduces the statistical support for the interaction model (Table S7).

For four stock combinations (piscivore stocks: Spotted spiny dogfish Pacific Coast, Pacific hake Pacific Coast, Atlantic cod Iceland, and Arrowtooth flounder Pacific Coast), the biomass of the forage-fish stock is lower than that of the piscivore stock (Fig. S4). Since this might indicate that the forage-fish stock is not large enough to singly support the piscivore stock, we tested the robustness of our results to the exclusion of these stock combinations (Fig. S4 and Table S6). The exclusion of these stock combinations does not reduce the statistical support for the interaction model, and in the main text we therefore show results with these stock combinations included.

Biomass declines at the start of time series can, when predicted by assessment models that estimate virgin biomass, be artifacts of the assessment-model assumptions. This is especially relevant when predicted declines occur prior to periods that

are covered by catch data and/or survey data. These problems are likely to be most prevalent before 1970. We therefore tested the robustness of our results to the exclusion of four stock combinations with continuous and long-lasting declines in piscivore biomass ocurring from the start of the time series with little spread in the individual data points (piscivore stocks: Arrowtooth flounder Pacific Coast, South hake Chile, Petrale sole Pacific Coast, and Yelloweye rockfish Pacific Coast); the results are shown in Table S11. In addition, we tested the robustness of our results to the exclusion of three stock combinations with declines in piscivore biomass starting prior to 1970 (piscivore stocks: Arrowtooth flounder Pacific Coast, Petrale sole Pacific Coast, and Spotted spiny dogfish Pacific Coast); the results are shown in Table S12. In both cases, the exclusion of these stock combinations does not reduce the statistical support for the interaction model, and in the main text we therefore show results with these stock combinations included.

Selection of period with strongest piscivore biomass decline. The length of periods with declining piscivore biomass varies among stocks (Fig. S1). Therefore, we allowed the selected period to vary between 5 and 15 years and tested for the robustness of our results against variation in the minimum and maximum length of this period (Tables S8-S10).

To determine the time periods over which the decline in piscivore biomass is the largest, we used three different methods. For the first two methods, we defined a decline in biomass as the ratio between the piscivore biomasses at the end and at the beginning of the period. The period with the strongest biomass decline in a time series is then taken as the period for which this ratio is the smallest. For the first method, the biomass ratio is calculated based on raw data of piscivore biomass. For the second method, the biomass ratio is calculated based on a smoothing spline fitted to the piscivore biomass data. The number of free knots used to derive the smoothing spline is 1/3 of the total number of years per stock (Fig. S1). For the third method, we fitted linear regression models to subranges of the piscivore biomass data. A decline in biomass is then defined as a negative regression slope, and the period of strongest biomass decline is taken as the period with the most negative regression slope. The main results (Fig. 4, Table 1 and S5) are based on the first method, i.e., on biomass ratios of raw piscivore biomass data.

Alternative data sources. The newest version of the RAM Legacy Stock Assessment Database (16) contains data on catch per unit effort (CPUE) from trawl surveys for two of the piscivore stocks in our analysis (Fig. S5). In addition, we derived CPUE information from eight bottom-trawl surveys for some other, European, piscivore stocks (Fig. S6). The data were taken from the ICES DATRAS (17) and processed following the methodology described by Maureaud et al. (18). Specifically, we used trawl-survey data from the North Sea International Bottom Trawl Survey, the Scottish West Coast International Bottom Trawl Survey, the French Southern Atlantic Bottom Trawl Survey, the Irish International Groundfish Survey, the French Channel Groundfish Survey, the Northern Ireland Groundfish Survey, the Portuguese International Bottom Trawl Survey, and the Baltic International Trawl Survey.

Several steps were needed to estimate relative changes in CPUE from the ICES trawl-survey data over time. First, the assessment region was selected for each piscivore stock by overlapping the bounding regions of the fisheries-assessment areas (19) with a 1-degree grid to obtain gridded assessment regions. Second, the trawl-survey coordinates were linked to the grid cells. Third, grid cells that contain one or more survey samples per year across the time series were selected, and grid cells that were infrequently sampled (<3 times since 1980) were removed. Fourth, the average CPUE was calculated over cells per year by averaging over all sampling locations in each grid cell and then across the grid over cells. Some fisheries-assessment areas overlapped with multiple surveys, in which case the average CPUE was estimated for the entire region. The averaging resulted in an estimate of how the CPUE changes over time, which was compared to the stock-assessment data. For some stocks, trawl-survey data was available for longer periods, but no CPUE could be calculated. This occurred because the swept area (defined by the trawl's wing spread or door spread multiplied by the sampled distance) could not be estimated from the available data or because estimates of the weight of caught fish were not reported. For three other stocks, no CPUE data was available, and we instead show time series of average trawl-survey-based catches (Fig. S6). All trawl-survey-based estimates were manually rescaled to overlap with the stock-assessment-based values in the same time periods (this rescaling is immaterial for our analyses as only relative changes in biomass over time are used in our analysis).

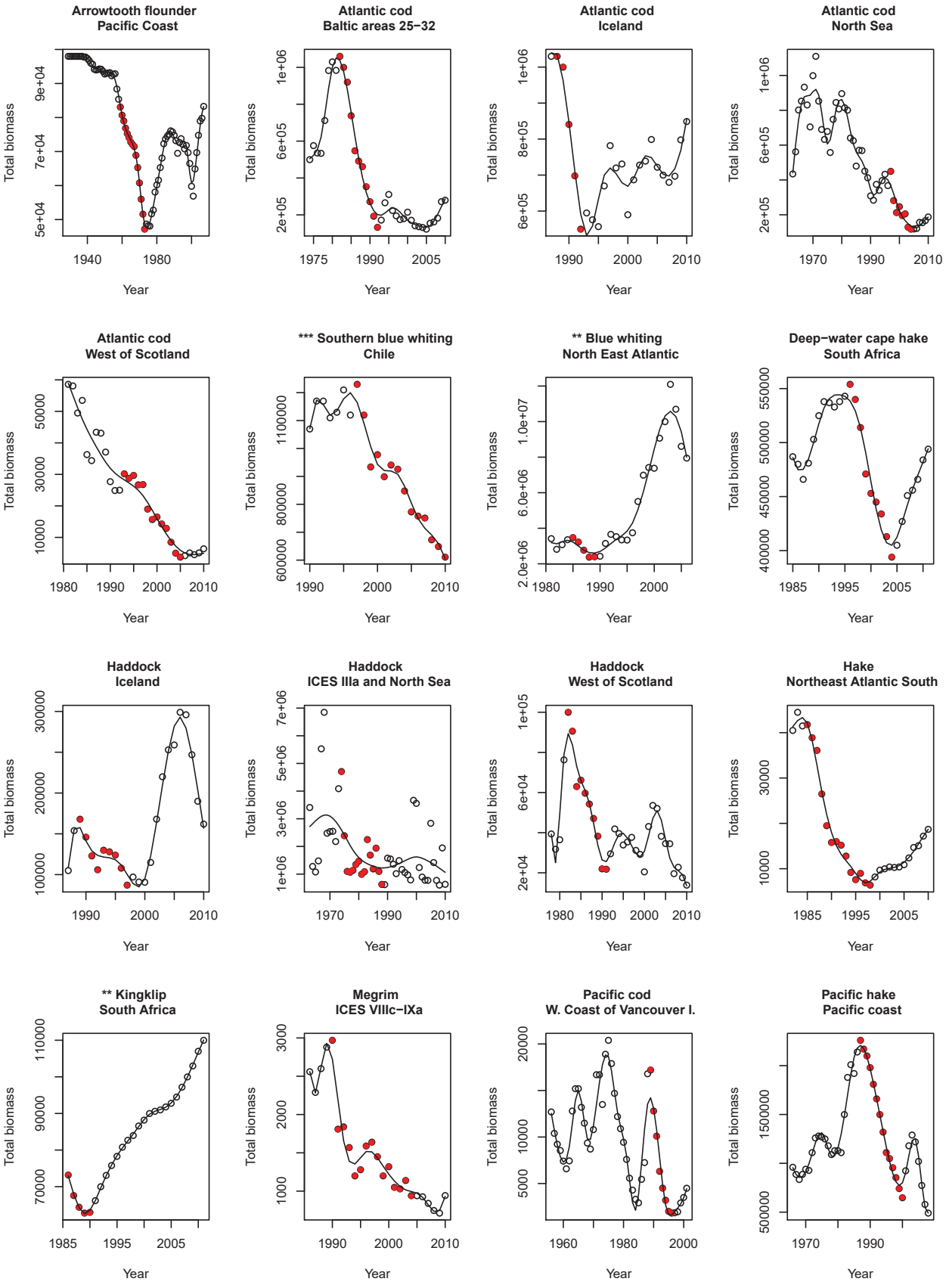
Arrowtooth flounder
Pacific Coast
Atlantic cod
Baltic areas 25−32
Atlantic cod
Iceland
Atlantic cod
North Sea
Atlantic cod
West of Scotland
*** Southern blue whiting
Chile
** Blue whiting
North East Atlantic
Deep−water cape hake
South Africa
Haddock
Iceland
Haddock
ICES IIIa and North Sea
Haddock
West of Scotland
Hake
Northeast Atlantic South
** Kingklip
South Africa
Megrim
ICES VIIIc−IXa
Pacific cod
W. Coast of Vancouver I.
Pacific hake
Pacific coast
Total biomass
Year

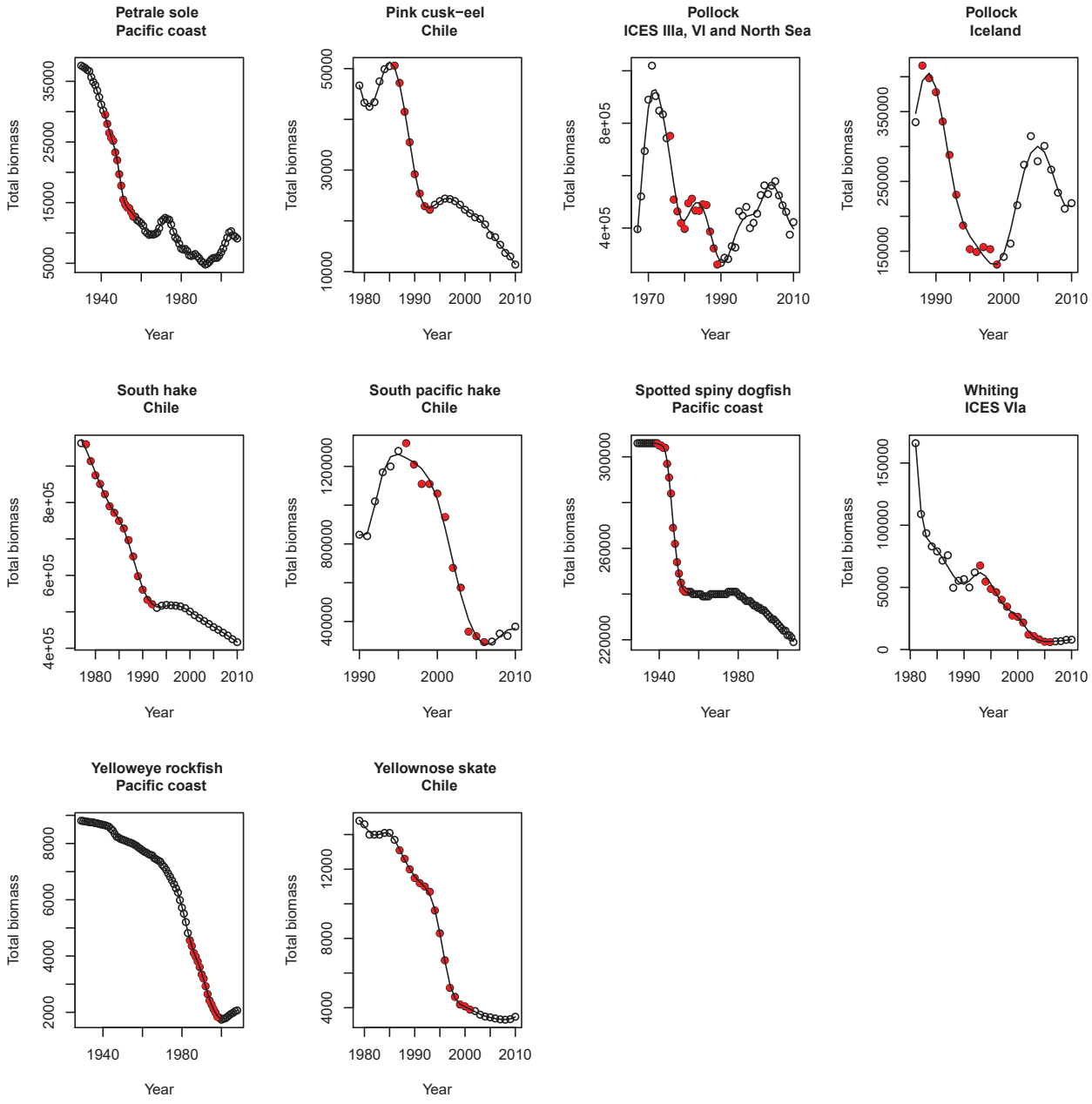

Fig. S1. Biomass time series of all piscivore stocks (open circles; in metric tons) and periods with strongest piscivore-biomass decline (red dots; the periods are allowed to vary between 5 and 15 years). This data is used to produce Figure 4 and Tables 1 and S5. The black lines represent the smoothing splines used to determine the periods with strongest piscivore-biomass decline as shown in Table S9. We excluded four piscivore stocks marked with ** because their biomass was predominantly increasing, as well as the single piscivore stock marked with *** because it had a strong influence on the interaction model (Fig. S3, Table S7).

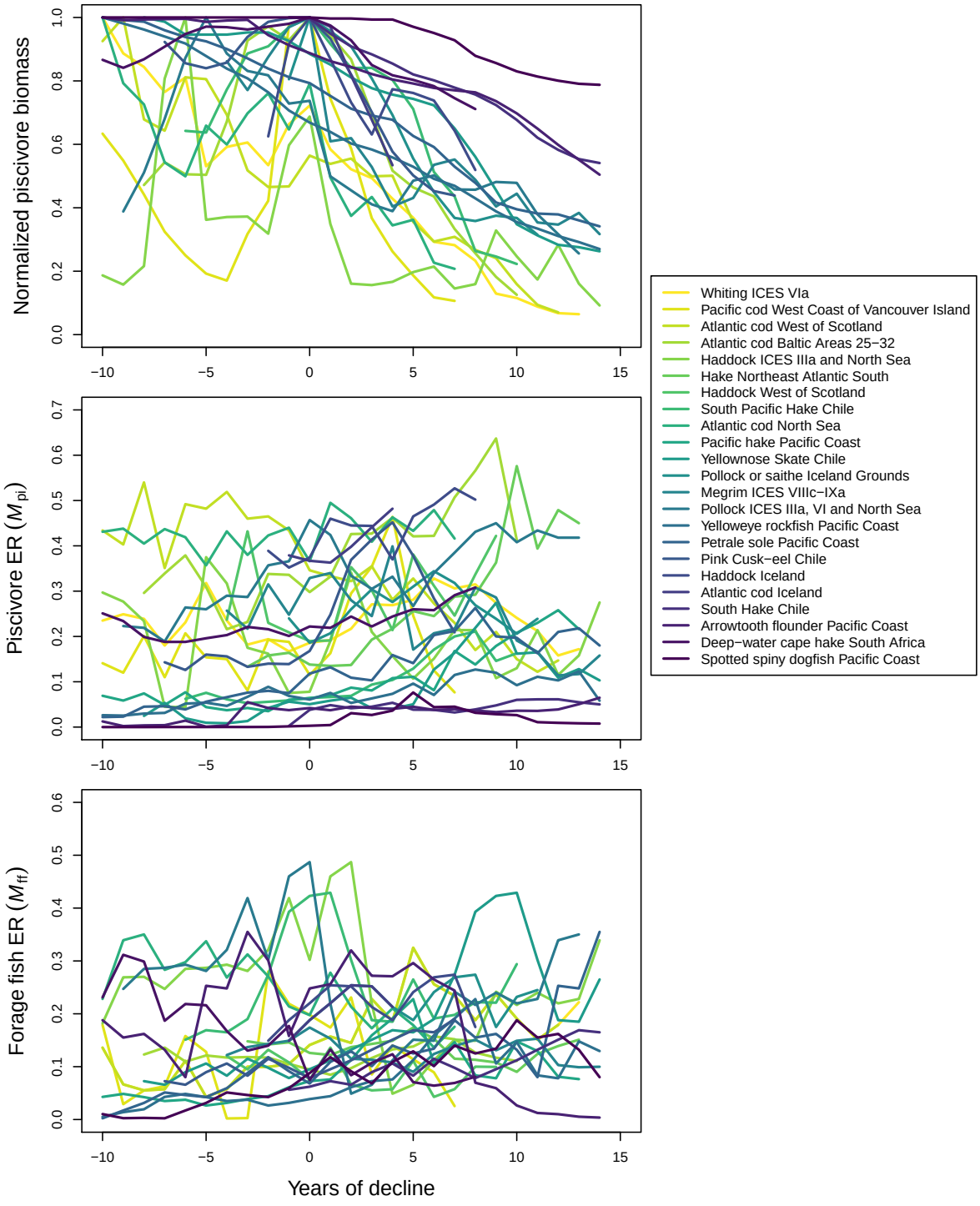

Fig. S2. Trends in piscivore biomass and fishing mortality of piscivore and forage-fish stocks that were linked to the piscivore stocks, during the 10 years prior to the selected period of strongest piscivore-biomass decline. Piscivore biomass is normalized by dividing by the maximum biomass in each time series. Fishing mortality is measured by the exploitation rate (annual catch/stock biomass), abbreviated by ER and denoted by M_{pi} for piscivores and M_{ff} for forage fish.

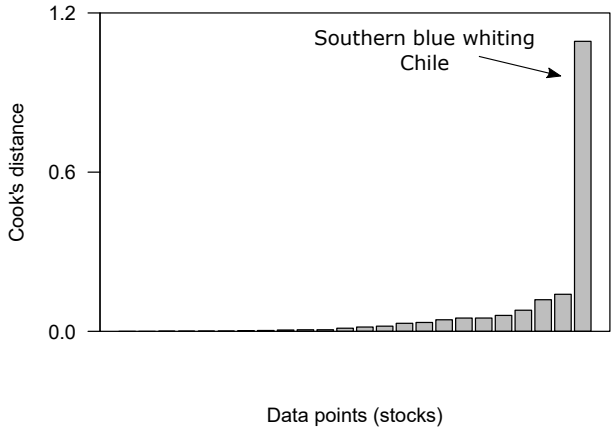

Fig. S3. Cook's distances for all considered stock combinations, which measure the effect of deleting an observation. The stock combination with the piscivore stock 'Southern Blue whiting Chile' has a much larger Cook's distance than all other stock combinations, and therefore all analyses were done without this stock combination.

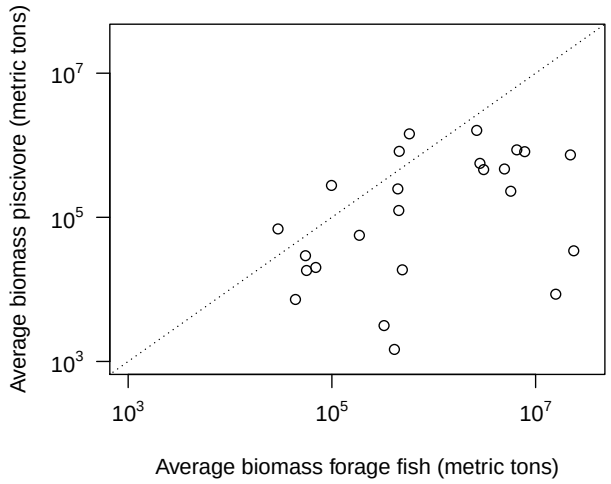

Fig. S4. Average biomass of piscivore and forage-fish stocks for the selected periods of strongest piscivore-biomass decline. The diagonal represents the line along which piscivore biomass and forage-fish biomass are equal. For the four stock combinations (piscivore stocks: Spotted spiny dogfish Pacific Coast, Pacific hake Pacific Coast, Atlantic cod Iceland, and Arrowtooth flounder Pacific Coast) above the diagonal, the piscivore biomass exceeds the forage-fish biomass.

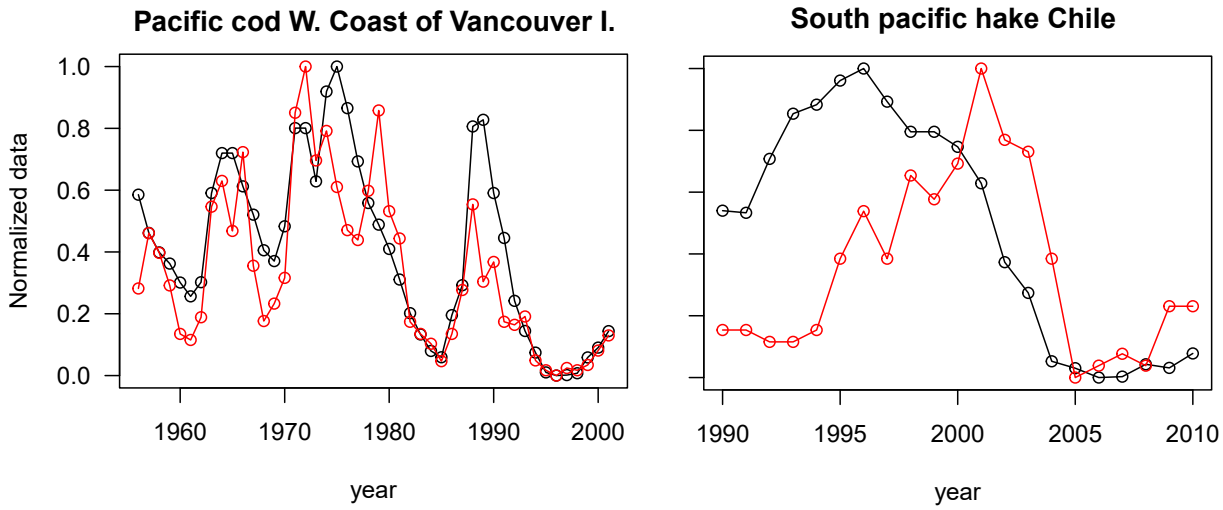

Fig. S5. Comparison of trawl-survey-based (red) and stock-assessment-based (black) stock-biomass estimates for two of the piscivore stocks included in our analysis, from the RAM Legacy Stock Assessment Database (16). Both time series are normalized to the unit interval according to their minimum and maximum values.

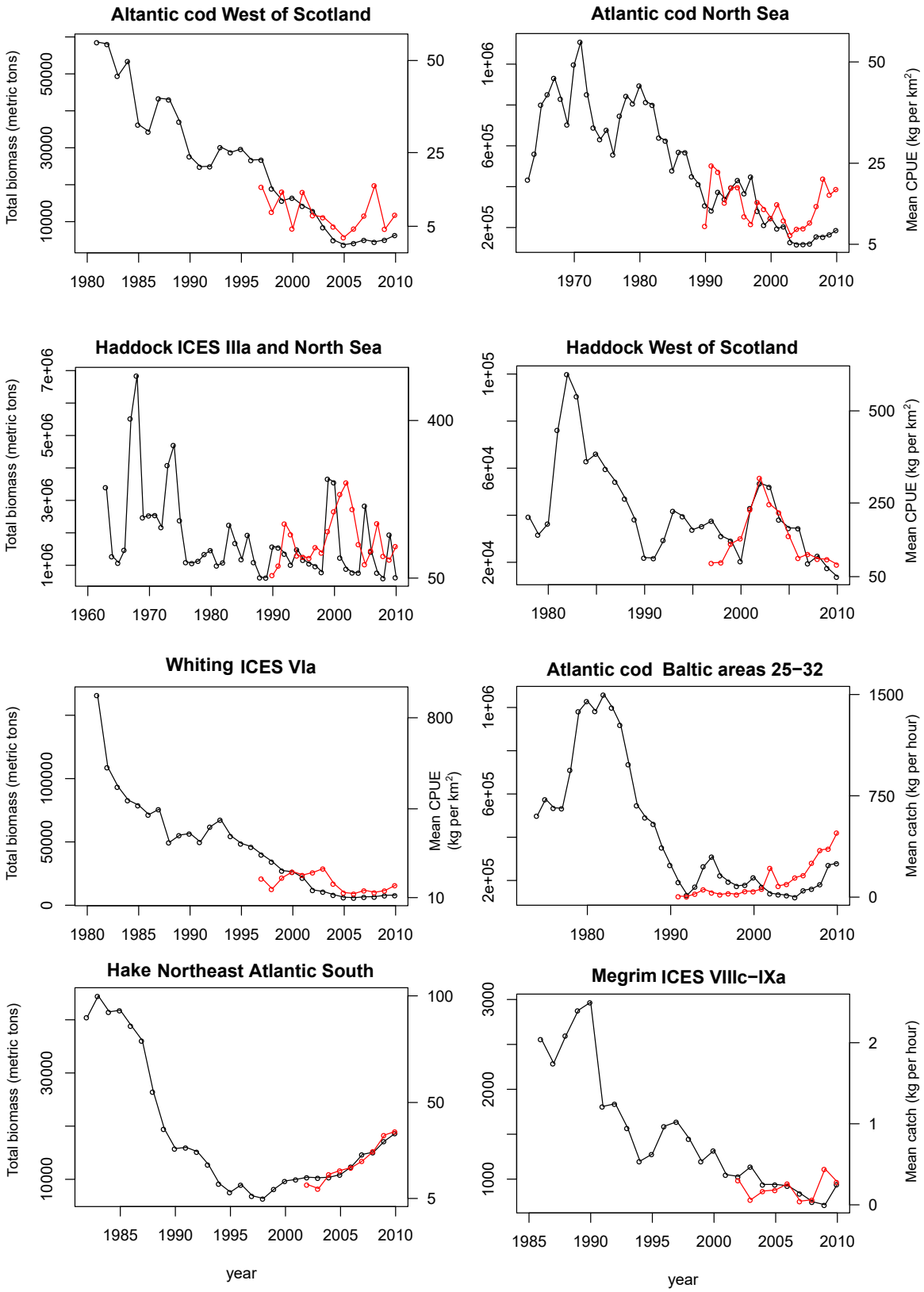

Fig. S6. Comparison of trawl-survey-based (red) and stock-assessment-based (black) stock-biomass estimates. The trawl-survey-based estimates are available only for a small part of the time series and were determined either according to catch per unit effort based on the area swept (CPUE; for the first five stocks) or according to catch per hour (for the last three stocks). Note that the two estimates are shown on different scales: the trawl-survey-based estimates were manually rescaled to overlap with the stock-assessment-based estimates in the same time period (this rescaling is immaterial for our analyses as only relative changes in biomass over time are used in our analysis).

Table S5. Overview of the combinations of piscivore stocks and forage-fish stocks used for the statistical model. The piscivore-biomass decline B_{pi} is measured as the ratio of piscivore biomasses at the end and at the beginning of the selected decline period (Fig. S1). Fishing mortalities M_{pi} and M_{ff} for, respectively, piscivores and forage fish are averaged over these decline periods. When multiple forage-fish stocks overlap with a single piscivore stock, aggregate forage-fish fishing mortalities were calculated as biomass-weighted averages. Fishing mortality is measured by the exploitation rate (annual catch/stock biomass). We excluded the forage-fish stock marked with * because it was doubly represented, four piscivore stocks marked with ** because their biomass was predominantly increasing, and the piscivore stock marked with * because it had a particularly strong influence on the interaction model (Fig. S3 and Table S7).**

Piscivore stocks						**Forage-fish stocks**			
Common name	**Stock location**	**Start**	**Period (yr)**	B_{pi}	M_{pi}	**Common name**	**Stock location**	M_{ff}	**Stocks**
Arrowtooth flounder	Pacific Coast	1959	15	0.57	0.04	Pacific chub mackerel	Pacific Coast	0.16	2
						Pacific sardine	Pacific Coast		
Atlantic cod	ICES Baltic Areas 25-32	1982	11	0.13	0.45	Sprat	ICES Baltic Areas 22-32	0.12	2
						Herring	ICES Baltic Areas 25-32		
Atlantic cod	Iceland	1988	5	0.53	0.41	Herring (summer spawners)	Iceland	0.23	1
Atlantic cod	North Sea	1997	8	0.26	0.44	Sandeel	North Sea Area 1	0.2	4
						Sandeel	North Sea Area 2		
						Sandeel	North Sea Area 3		
						Herring	North Sea		
Atlantic cod	West of Scotland	1993	13	0.12	0.25	Herring*	ICES Area VIa	0.16	2
						Herring	ICES Areas VIa-VIIb-VIIc		
Southern Blue whiting***	Chile	1997	14	0.5	0.04	Chilean jack mackerel	Chilean EEZ and offshore	0.28	1
Blue whiting**	North East Atlantic	1985	5	0.7	0.24	Mackerel	North East Atlantic	0.19	1
Deep-water cape hake	South Africa	1996	9	0.71	0.25	Sardine	South Africa	0.09	2
						Anchovy	South Africa		
Haddock	Iceland	1989	9	0.52	0.45	Herring (summer spawners)	Iceland	0.23	1
Haddock	ICES Area IIIa and North Sea	1974	15	0.13	0.18	Sandeel	North Sea Area 1	0.23	4
						Sandeel	North Sea Area 2		
						Sandeel	North Sea Area 3		
						Herring	North Sea		
Haddock	West of Scotland	1982	10	0.22	0.29	Herring*	ICES Area VIa	0.11	2
						Herring	ICES Areas VIa-VIIb-VIIc		
Hake	Northeast Atlantic South	1985	14	0.15	0.3	European pilchard	ICES Areas VIIIc-IXa	0.13	1
Kingklip**	South Africa	1986	5	0.86	0.11	Sardine	South Africa	0.25	2
						Anchovy	South Africa		
Megrim	ICES Areas VIIIc-IXa	1990	15	0.32	0.24	European pilchard	ICES Areas VIIIc-IXa	0.13	1
Pacific cod	West Coast of Vancouver Island	1989	8	0.11	0.23	Pacific herring	West Coast of Vancouver Island	0.13	1

Table S5. Continued.

Piscivore stocks						Forage-fish stocks			
Common name	**Stock location**	**Start**	**Period (yr)**	$B_{\mathbf{pi}}$	$M_{\mathbf{pi}}$	**Common name**	**Stock location**	$M_{\mathbf{ff}}$	**Stocks**
Pacific hake	Pacific Coast	1987	14	0.29	0.14	Pacific chub mackerel	Pacific Coast	0.12	2
						Pacific sardine	Pacific Coast		
Petrale sole	Pacific Coast	1942	15	0.43	0.17	Pacific chub mackerel	Pacific Coast	0.16	2
						Pacific sardine	Pacific Coast		
Pink cusk-eel	Chile	1986	8	0.44	0.32	Chilean jack mackerel	Chilean EEZ and offshore	0.14	1
Pollock	ICES Areas IIIa, VI and North Sea	1976	14	0.35	0.39	Sandeel	North Sea Area 1	0.22	4
						Sandeel	North Sea Area 2		
						Sandeel	North Sea Area 3		
						Herring	North Sea		
Pollock	Iceland	1988	12	0.31	0.26	Herring (summer spawners)	Iceland	0.23	1
South hake	Chile	1978	15	0.54	0.05	Chilean jack mackerel	Chilean EEZ and offshore	0.11	1
South Pacific hake	Chile	1996	11	0.22	0.13	Chilean jack mackerel	Chilean EEZ and offshore	0.27	1
Spotted spiny dogfish	Pacific Coast	1939	15	0.79	0.03	Pacific chub mackerel	Pacific Coast	0.12	2
						Pacific sardine	Pacific Coast		
Whiting	ICES Area VIa	1993	14	0.09	0.24	Herring*	ICES Area VIa	0.17	2
						Herring	ICES Areas VIa-VIIb-VIIc		
Yelloweye rockfish	Pacific Coast	1984	15	0.4	0.09	Pacific chub mackerel	Pacific Coast	0.11	2
						Pacific sardine	Pacific Coast		
Yellownose skate	Chile	1987	15	0.3	0.12	Chilean jack mackerel	Chilean EEZ and offshore	0.23	1

Table S6. Effects of the exclusion of four stock combinations (piscivore stocks: Spotted spiny dogfish Pacific Coast, Pacific hake Pacific Coast, Atlantic cod Iceland, and Arrowtooth flounder Pacific Coast) with low forage-fish biomasses (compared to Table 1) on alternative statistical models of the effects of piscivore and forage-fish fishing on piscivore-biomass declines. The piscivore-biomass decline $B_{\mathbf{pi}}$ is measured as the ratio of piscivore biomasses at the end and at the beginning of the selected decline periods (Fig. S1). The models describe the logarithmic decline as a function of the average piscivore fishing mortality $M_{\mathbf{pi}}$ and the average forage-fish fishing mortality $M_{\mathbf{ff}}$ during the decline period. Fishing mortality is measured by the exploitation rate (annual catch/stock biomass). 19 combinations of piscivore stocks and forage-fish stocks were included in this analysis. p_1, p_2, and p_3 show the p-values for the regression coefficients of, respectively, the model terms $M_{\mathbf{pi}}$, $M_{\mathbf{ff}}$, and $M_{\mathbf{pi}}M_{\mathbf{ff}}$. r^2 is the coefficient of determination (adjusted r^2), SE is the standard error of the intercept and the regression coefficients, AIC is the AIC score, and $\triangle$AIC is the difference in AIC score relative to the model with the minimal AIC score.

Model	p-value	SE	r^2	AIC	$\triangle$AIC
$\ln(B_{\text{pi}}) = 0.8 - 7.9\,M_{\text{pi}} - 11.8\,M_{\text{ff}} + 42.6\,M_{\text{pi}}M_{\text{ff}}$	p_1 = 0.05	1.0	0.11	38.5	0
	p_2 = 0.04	3.7			
	p_3 = 0.05	5.3			
		20.4			
$\ln(B_{\text{pi}}) = -0.9 - 0.5\,M_{\text{pi}} - 1.9\,M_{\text{ff}}$	p_1 = 0.69	0.5	-0.05	41.3	2.8
	p_2 = 0.47	1.3			
		2.6			
$\ln(B_{\text{pi}}) = -1.2 - 0.6\,M_{\text{pi}}$	p_1 = 0.65	0.3	-0.08	39.9	1.6
		1.2			

Table S7. Effects of the inclusion of Blue whiting Chile (compared to Table 1) on alternative statistical models of the effects of piscivore and forage-fish fishing on piscivore-biomass declines. The piscivore-biomass decline $B_{\mathbf{pi}}$ is measured as the ratio of piscivore biomasses at the end and at the beginning of the selected decline periods (Fig. S1). The models describe the logarithmic decline as a function of the average piscivore fishing mortality $M_{\mathbf{pi}}$ and the average forage-fish fishing mortality $M_{\mathbf{ff}}$ during the decline period. Fishing mortality is measured by the exploitation rate (annual catch/stock biomass). 24 combinations of piscivore stocks and forage-fish stocks were included in this analysis. p_1, p_2, and p_3 show the p-values for the regression coefficients of, respectively, the model terms $M_{\mathbf{pi}}$, $M_{\mathbf{ff}}$, and $M_{\mathbf{pi}}M_{\mathbf{ff}}$. r^2 is the coefficient of determination (adjusted r^2), SE is the standard error of the intercept and the regression coefficients, AIC is the AIC score, and $\triangle$AIC is the difference in AIC score relative to the model with the minimal AIC score.

Model	p-value	SE	r^2	AIC	$\triangle$AIC
$\ln(B_{\text{pi}}) = 0.3 - 6.6\,M_{\text{pi}} - 6.6\,M_{\text{ff}} + 29.8\,M_{\text{pi}}M_{\text{ff}}$	p_1 = 0.04	0.7	0.09	49.1	0.1
	p_2 = 0.10	3.1			
	p_3 = 0.08	3.8			
		16.1			
$\ln(B_{\text{pi}}) = -0.8 - 1.2\,M_{\text{pi}} - 0.8\,M_{\text{ff}}$	p_1 = 0.22	0.5	-0.01	51.0	1.9
	p_2 = 0.73	1.0			
		2.2			
$\ln(B_{\text{pi}}) = -0.9 - 1.2\,M_{\text{pi}}$	p_1 = 0.20	0.3	0.03	49.0	0
		1.0			

Table S8. Effects of different minimum and maximum durations of the periods of strongest piscivore-biomass decline (compared to Table 1) on model selection for the effects of piscivore and forage-fish fishing on piscivore-biomass declines. The piscivore-biomass decline $B_{\mathbf{pi}}$ is measured as the ratio of piscivore biomasses at the end and at the beginning of the selected decline periods (Fig. S1). The models describe the logarithmic decline as a function of the average piscivore fishing mortality $M_{\mathbf{pi}}$ and the average forage-fish fishing mortality $M_{\mathbf{ff}}$ during the decline period. Fishing mortality is measured by the exploitation rate (annual catch/stock biomass). The best model is selected on the basis of AIC scores; the model with the fewest degrees of freedom is selected when the differences in AIC scores are < 2. 23 combinations of piscivore stocks and forage-fish stocks were included in this analysis. F indicates that a full model, $\ln(B_{\mathbf{pi}}) = a + b\,M_{\mathbf{pi}} + c\,M_{\mathbf{ff}} + d\,M_{\mathbf{pi}}M_{\mathbf{ff}}$, has the minimal AIC score. The coefficient of determination is shown in parentheses (adjusted r^2); best models with an r^2 below 0.05 are not shown (indicated by '-').

		Maximum length (yr)											
		8	9	10	11	12	13	14	15	16	17	18	19
Minimum length (yr)	5	-	F (0.29)	F (0.32)	F (0.32)	F (0.35)	F (0.31)	F (0.28)	F (0.26)	F (0.29)	F (0.17)	-	F (0.18)
	6	F (0.19)	F (0.29)	F (0.32)	F (0.32)	F (0.34)	F (0.30)	F (0.26)	F (0.25)	F (0.27)	-	-	-
	7	F (0.23)	F (0.30)	F (0.33)	F (0.33)	F (0.35)	F (0.31)	F (0.27)	F (0.25)	F (0.29)	-	-	-
	8		F (0.29)	F (0.33)	F (0.33)	F (0.35)	F (0.31)	F (0.27)	F (0.25)	F (0.29)	-	-	-
	9			F (0.32)	F (0.32)	F (0.33)	F (0.30)	F (0.26)	F (0.27)	F (0.27)	-	-	-
	10				F (0.33)	F (0.35)	F (0.32)	F (0.28)	F (0.28)	F (0.28)	-	-	F (0.18)
	11					F (0.34)	F (0.29)	F (0.28)	F (0.26)	F (0.26)	-	-	F (0.18)
	12						F (0.21)	F (0.28)	F (0.27)	F (0.28)	-	F (0.18)	F (0.20)
	13							F (0.29)	F (0.27)	F (0.26)	-	-	F (0.19)
	14								F (0.23)	F (0.25)	-	-	F (0.17)

Table S9. Effects of processing the raw time series through smoothing (compared to Table S8) on model selection for the effects of piscivore and forage-fish fishing on piscivore-biomass declines. The piscivore-biomass decline $B_{\mathbf{pi}}$ is measured as the ratio of biomasses at the end and at the beginning of the selected decline periods based on a smoothing spline fitted to the piscivore-biomass data (Fig. S1). The minimum and maximum durations of the period of strongest piscivore-biomass decline were varied. The models describe the logarithmic decline as a function of the average piscivore fishing mortality $M_{\mathbf{pi}}$ and the average forage-fish fishing mortality $M_{\mathbf{ff}}$ during the decline period. Fishing mortality is measured by the exploitation rate (annual catch/stock biomass). The best model is selected on the basis of AIC scores; the model with the fewest degrees of freedom is selected when the differences in AIC scores are < 2. 23 combinations of piscivore stocks and forage-fish stocks were included in this analysis. F indicates that a full model, $\ln(B_{\mathbf{pi}}) = a + b\,M_{\mathbf{pi}} + c\,M_{\mathbf{ff}} + d\,M_{\mathbf{pi}}M_{\mathbf{ff}}$, has the minimal AIC score, whereas S indicates that a simple model, $\ln(B_{\mathbf{pi}}) = a + b\,M_{\mathbf{pi}}$, has the minimal AIC score. The coefficient of determination is shown in parentheses (adjusted r^2); best models with an r^2 below 0.05 are not shown (indicated by '-').

		Maximum length (yr)											
		8	9	10	11	12	13	14	15	16	17	18	19
Minimum length (yr)	5	S (0.06)	-	F (0.20)	S (0.07)	-	-	-	-	-	-	-	-
	6	-	-	F (0.18)	F (0.26)	-	-	-	-	F (0.18)	-	-	-
	7	-	-	F (0.30)	F (0.26)	-	-	-	-	F (0.18)	-	-	-
	8		F (0.22)	F (0.30)	F (0.26)	-	-	-	-	F (0.18)	-	-	-
	9			F(0.39)	F (0.33)	S (0.06)	-	-	F (0.19)	F (0.22)	-	-	-
	10				F (0.32)	S (0.05)	-	-	F (0.21)	F (0.22)	-	-	-
	11					-	-	-	F (0.19)	F (0.20)	-	-	-
	12						-	-	F (0.20)	F (0.21)	-	-	-
	13							F (0.17)	F (0.19)	F (0.20)	-	-	-
	14								F (0.20)	F (0.16)	-	-	-

Table S10. Effects of processing the raw time series through regression (compared to Table S8) on model selection for the effects of piscivore and forage-fish fishing on piscivore-biomass declines. The piscivore-biomass decline B_{pi} is measured as the ratio of biomasses at the end and at the beginning of the selected decline periods based on a linear regression fitted to the piscivore-biomass data. The minimum and maximum durations of the period of strongest piscivore-biomass decline were varied. The models describe the logarithmic decline as a function of the average piscivore fishing mortality M_{pi} and the average forage-fish fishing mortality M_{ff} during the decline period. Fishing mortality is measured by the exploitation rate (annual catch/stock biomass). The best model is selected on the basis of AIC scores; the model with the fewest degrees of freedom is selected when differences in AIC scores are < 2. 23 combinations of piscivore stocks and forage-fish stocks were included in this analysis. F indicates that a full model, $\ln(B_{pi}) = a + b\,M_{pi} + c\,M_{ff} + d\,M_{pi}M_{ff}$, has the minimal AIC score, whereas S indicates that a simple model, $\ln(B_{pi}) = a + b\,M_{pi}$, has the minimal AIC score. The coefficient of determination is shown in parentheses (adjusted r^2); best models with an r^2 below 0.05 are not shown (indicated by '-').

		Maximum length (yr)											
		8	9	10	11	12	13	14	15	16	17	18	19
Minimum length (yr)	5	S (0.07)	S (0.07)	S (0.07)	S (0.07)	S (0.07)	S (0.07)	S (0.07)	S (0.07)	S (0.07)	S (0.07)	S (0.07)	S (0.07)
	6	-	-	-	-	-	-	-	-	-	-	-	-
	7	-	-	-	-	-	-	-	-	-	-	-	-
	8		-	-	-	-	-	-	-	-	-	-	-
	9			-	-	-	-	-	-	-	-	-	-
	10				F (0.20)	F (0.20)	F (0.20)	F (0.20)	F (0.20)	F (0.20)	F (0.20)	F (0.20)	F (0.20)
	11					F (0.25)	F (0.25)	F (0.25)	F (0.25)	F (0.25)	F (0.25)	F (0.25)	F (0.25)
	12						F (0.22)	F (0.22)	F (0.22)	F (0.22)	F (0.22)	F (0.22)	F (0.22)
	13							F (0.17)	F (0.17)	F (0.17)	F (0.17)	F (0.17)	F (0.17)
	14								F (0.18)	F (0.18)	F (0.18)	F (0.18)	F (0.18)

Table S11. Effects of the exclusion of four stock combinations (piscivore stocks: Arrowtooth flounder Pacific Coast, South hake Chile, Petrale sole Pacific Coast, and Yelloweye rockfish Pacific Coast) with declines early in the time series (compared to Table 1) on alternative statistical models of the effects of piscivore and forage-fish fishing on piscivore-biomass declines. The piscivore-biomass decline B_{pi} is measured as the ratio of piscivore biomasses at the end and at the beginning of the selected decline periods (Fig. S1). The models describe the logarithmic decline as a function of the average piscivore fishing mortality M_{pi} and the average forage-fish fishing mortality M_{ff} during the decline period. Fishing mortality is measured by the exploitation rate (annual catch/stock biomass). 19 combinations of piscivore stocks and forage-fish stocks were included in this analysis. p_1, p_2, and p_3 show the p-values for the regression coefficients of, respectively, the model terms M_{pi}, M_{ff} and $M_{pi}M_{ff}$. r^2 is the coefficient of determination (adjusted r^2), SE is the standard error of the intercept and the regression coefficients, AIC is the AIC score, and $\triangle$AIC is the difference in AIC score relative to the model with the minimal AIC score.

Model	p-value	SE	r^2	AIC	$\triangle$AIC
$\ln(B_{pi}) = 1.3 - 10.0\,M_{pi} - 14.4\,M_{ff} + 54.4\,M_{pi}M_{ff}$	p_1 = 0.03	1.1	0.16	39.4	0
	p_2 = 0.03	4.1			
	p_3 = 0.02	5.9			
		21.5			
$\ln(B_{pi}) = -1.2 - 0.1\,M_{pi} - 1.0\,M_{ff}$	p_1 = 0.95	0.6	-0.12	44.1	4.7
	p_2 = 0.74	1.3			
		2.8			
$\ln(B_{pi}) = -1.3 - 0.1\,M_{pi}$	p_1 = 0.93	0.4	-0.06	42.2	2.9
		1.3			

Table S12. Effects of the exclusion of three stock combinations (piscivore stocks: Petrale sole Pacific Coast, Arrowtooth flounder, Pacific Coast, and Spotted spiny dogfish Pacific Coast) with declines starting prior to 1970 (compared to Table 1) on alternative statistical models of the effects of piscivore and forage-fish fishing on piscivore-biomass declines. The piscivore-biomass decline B_{pi} is measured as the ratio of piscivore biomasses at the end and at the beginning of the selected decline periods (Fig. S1). The models describe the logarithmic decline as a function of the average piscivore fishing mortality M_{pi} and the average forage-fish fishing mortality M_{ff} during the decline period. Fishing mortality is measured by the exploitation rate (annual catch/stock biomass). 20 combinations of piscivore stocks and forage-fish stocks were included in this analysis. p_1, p_2, and p_3 show the p-values for the regression coefficients of, respectively, the model terms M_{pi}, M_{ff}, and $M_{\mathrm{pi}}M_{\mathrm{ff}}$. r^2 is the coefficient of determination (adjusted r^2), SE is the standard error of the intercept and the regression coefficients, AIC is the AIC score, and $\triangle$AIC is the difference in AIC score relative to the model with the minimal AIC score.

Model	p-value	SE	r^2	AIC	$\triangle$AIC
$\ln(B_{\mathrm{pi}}) = 0.7 - 8.0\,M_{\mathrm{pi}} - 12.1\,M_{\mathrm{ff}} + 46.1\,M_{\mathrm{pi}}M_{\mathrm{ff}}$	p_1 = 0.03	0.9	0.15	39.1	0
	p_2 = 0.03	3.5			
	p_3 = 0.03	5.0			
		18.8			
$\ln(B_{\mathrm{pi}}) = -1.2 - 0.1\,M_{\mathrm{pi}} - 1.2\,M_{\mathrm{ff}}$	p_1 = 0.95	0.5	-0.10	43.5	4.4
	p_2 = 0.64	1.2			
		2.5			
$\ln(B_{\mathrm{pi}}) = -1.3 - 0.01\,M_{\mathrm{pi}}$	p_1 = 0.99	0.3	-0.06	41.7	2.6
		1.0			

References

1. Yodzis P, Innes S (1992) Body size and consumer-resource dynamics. *American Naturalist* 139(6):1151–1175.
2. de Roos AM, et al. (2007) Food-dependent growth leads to overcompensation in stage-specific biomass when mortality increases: The influence of maturation versus reproduction regulation. *American Naturalist* 170(3):E59–E76.
3. Soudijn FH, de Roos AM (2017) Approximation of a physiologically structured population model with seasonal reproduction by a stage-structured biomass model. *Theoretical Ecology* 10(1):73–90.
4. van Leeuwen A, de Roos AM, Persson L (2008) How cod shapes its world. *Journal of Sea Research* 60(1):89–104.
5. Kuikka S, Hildén M (1999) Modeling environmentally driven uncertainties in Baltic cod (*Gadus morhua*) management by Bayesian influence diagrams. *Canadian Journal of Fisheries and Aquatic Science* 56(4):629–641.
6. FishBase (2015) *Length-weight relationships of Clupea harengus*. eds. Froese R, Pauly D. (https://www.fishbase.se/summary/24).
7. Kuikka S, Suuronen P, Parmanne R (1996) The impacts of increased codend mesh size on the northern Baltic herring fishery: Ecosystem and market uncertainties. *ICES Journal of Marine Science* 53(4):723–730.
8. ICES (2014) *Report of the Baltic Fisheries Assessment Working Group (WGBFAS)*. ICES CM 2014/ACOM: 10, 3-10 April 2014, Copenhagen.
9. Wieland K (2000) Changes in the timing of spawning of Baltic cod: Possible causes and implications for recruitment. *ICES Journal of Marine Science* 57(2):452–464.
10. Köster FW, et al. (2003) Recruitment of Baltic cod and sprat stocks: Identification of critical life stages and incorporation of environmental variability into stock-recruitment relationships. *Scientia Marina* 67(S1):129–154.
11. de Roos AM, Persson L (2013) Population and community ecology of ontogenetic development, in *Monographs in Population Biology, Volume 51*, eds. Levin SA, Horn HS. (Princeton University Press, Princeton and Oxford).
12. Ricard D, Minto C, Jensen OP, Baum JK (2012) Examining the knowledge base and status of commercially exploited marine species with the RAM Legacy Stock Assessment Database. *Fish and Fisheries* 13(4):380–398.
13. Essington TE, et al. (2015) Fishing amplifies forage fish population collapses. *Proceedings of the National Academy of Sciences of the USA* 112(21):201422020.
14. Boettiger C, Chamberlain S (2015) *R Interface to Fishbase*. (https://github.com/ropensci/rfishbase).
15. United Nations (1982) *United Nations Convention of the Law of the Sea (UNCLOS)*. (https://www.un.org/depts/los/convention_agreements/convention_overview_convention.htm).
16. RAM Legacy Stock Assessment Database (2018) *RAM Legacy Stock Assessment Database Version v4.4*. (http://doi.org/10.5281/zenodo.2542919).
17. ICES (2020) *ICES Database of Trawl Surveys (DATRAS)*. (https://datras.ices.dk).
18. Maureaud A, et al. (2019) Biodiversity–ecosystem functioning relationships in fish communities: Biomass is related to evenness and the environment, not to species richness. *Proceedings of the Royal Society B: Biological Sciences* 286(1906):20191189.
19. Rising J, Heal G (2014) Global benefits of marine protected areas. *NBER Working Paper Series No. 19982*. (National Bureau of Economic Research, Cambridge, MA, USA.)